RSC Advances

ROYAL SOCIETY OF CHEMISTRY

www.rsc.org/advances

TOC graphic

Ag nanoplates were obtained in our developed benzyl alcohol system in the presence of Al^{3+} ions or Fe^{3+} ions.

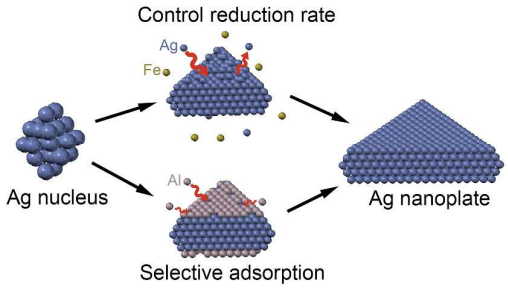

Journal Name RSCPublishing

COMMUNICATION

Effect of metal ions on the morphology of silver nanocrystals

Cite this: DOI: 10.1039/x0xx00000x

Gao Ming,[a] Ma Liran,[a] Gao Yuan,[a] Guo Dan,[a] Wang Dingsheng,[b] and Luo Jianbin*[a]

Received 00th January 2012,
Accepted 00th January 2012

DOI: 10.1039/x0xx00000x

www.rsc.org/

We developed a facile synthesis based on benzyl alcohol for Ag NCs. The effect of metal ions on the formation of silver nanocrystals was investigated. Ag nanoplates were obtained with the assistance of Al^{3+} ions or Fe^{3+} ions, while other metal ions had no influence and nanoparticles were produced instead.

Shape control for metallic nanostructures has been the focus of intensive research for decades due to their widespread applications in optics, electronics, magnetics, catalysis, and the intrinsic properties of metal nanocrystals have been demonstrated to depend on their exact size and morphology[1-5].Compared with other noble metal nanostructure, silver nanoparticles are of especial note because of their unique and tunable surface-plasmonic features, which promise a superior performance in many fields.

Over the past decades, different shapes of silver nanoparticles have been obtained via various syntheses, including spheres, disks, stars, rods, wires, prisms, cubes and right bipyramids[6-10]. More recently, silver nanoplates, as a two-dimensional anisotropic structure deviated from thermodynamics with sharp corners and edges, have particularly attracted our attention due to their fascinating optical properties[11] and intensive use such as SERS detectio[12], near-field optical probes[13], chemical and biological sensing[14]. Recently, a number of various routes have been developed to tune the size and thickness for plate-like structure, such as templating methods[15], electrochemical synthesis[16], photo-induced process[17-19], and direct chemical reduction[20].

The essential to form the extremely anisotropic plate-like structure is to overcome the thermodynamical tendency for minimizing the surface energy. A generic approach is to guarantee the slow formation rate for the nuclei and growth thus it could develop into the seed with stacking faults and covered by {111} facets at the top and bottom surfaces[8]. To achieve this goal, controlling kinetics is generally necessary[21]. One method is using a weak reducing agent to slow down the reduction rate. For example, Ag triangular nanoplates were produced by controlling the ratio of polyvinylpyrrolidone (PVP) whose hydroxyl end groups were found to serve as a grand weak reducing agent, it could also ensure the crystal growth slow enough[22]. Another method is to introduce an oxidation procedure into the reduction. It had been demonstrated that the suitable utilization of the oxidative power of H_2O_2 could produce silver nanoplates through the formation of planar twinned defects and elimination of other less stable structure[23]. In addition to employing of different reducing agents and oxidant, another strategy is to realize preferential anisotropic growth through selectively capping agents like surfactant, polymer, or small molecules, they could bind to a specific nanocrystallic facet, and simultaneously change the migration rate of that facet during nanocrystallic growth, resulting in plate-like structure.

However, among all morphology-tuned approaches, employ of foreign metal ions had been well-documented in literature of silver nanocrystal synthesis. For example, the impact of Cu^{+} ions or Cu^{2+} ions chloride in the silver polyol synthesis had been reported. It was found that ethylene glycol (EG) could reduce the Cu^{2+} to Cu^{+}, which effectively prevented oxygen atoms from absorbing on the surface of silver nanoparticles, while Cl^{-} controlled the saturation of free Ag^{+} and slowing the growth of seeds down, finally silver nanowires structure was generated[24]. In the present work, we systematically investigated the influence of various foreign metal ions on the nucleation and growth of silver nanocrystals in benzyl alcohol (BnOH) based synthetic system. We found that, distinctively, the presence of Al^{3+} ions or Fe^{3+} ions can successfully lead to the formation of silver nanoplates.

In a typical solvothermal synthesis, silver trifluoroacetate (CF_3COOAg) and PVP (M_w≈10,000) were dissolved in the reaction solution, in which BnOH was used as the solvent and mild reducing agent. Different metal ions such as Mg^{2+}, Al^{3+}, Fe^{3+}, Ni^{2+}, Zn^{2+}, Zr^{4+}, etc. were added into the solution, and the total volume was fixed at 5 ml. The mixture was stirring for 10 min in the air at room temperature. Afterward, the solution was heated to 120 ℃ for 6 h (detailed information about the procedures can be found in the Supporting Information, SI).

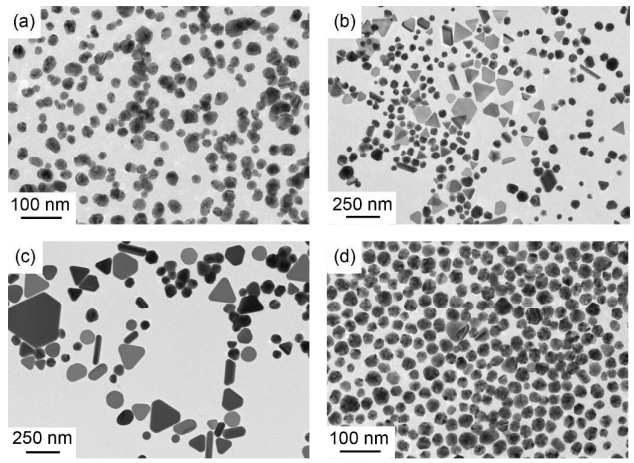

Figure 1. TEM micrographs of the AgNPs obtained by reacting CF_3COOAg with BnOH at 120 ℃ in different conditions. (a) in the presence of PVP alone. (b) in the presence of PVP and $Al(NO_3)_3{\cdot}9H_2O$ (c) in the presence of PVP and $Fe(NO_3)_3{\cdot}9H_2O$ (d) in the presence of PVP and $Mg(NO_3)_3{\cdot}6H_2O$.

The TEM images of final obtained silver nanocrystals are shown in Figure 1. As displayed in Figure 1a, without any foreign metal ions, the final product was quasi-spherical nanoparticles, whose size is 20-40 nm. Figure 1 b-d display the nanostructures synthesized with the described metal nitrates. It was evident the addition of $Fe(NO_3)_3{\cdot}9H_2O$ or $Al(NO_3)_3{\cdot}9H_2O$ could facilitate the formation of Ag nanoplates, with the yield to be 40% and 20%, respectively. Contrasting the shape and size, it is obvious to notice $Al(NO_3)_3{\cdot}9H_2O$ leading to more uniform triangular plate nanostructure while the $Fe(NO_3)_3{\cdot}9H_2O$ leading to diverse structures

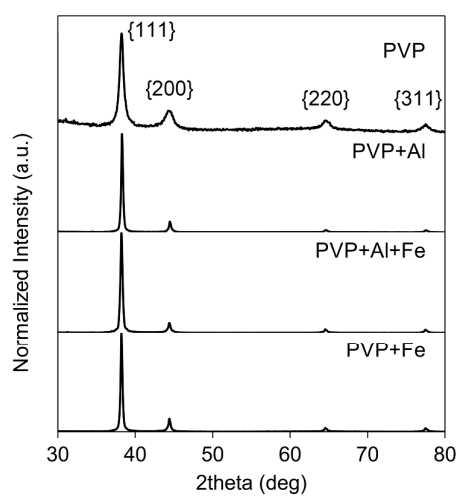

including nanodisks and triangular nanoplates.

Figure 2. XRD patterns of the Ag NCs obtained in the presence of PVP and different salts, as marked, Al corresponds to

$Al(NO_3)_3 \cdot 9H_2O$ and Fe corresponds to $Fe(NO_3)_3 \cdot 9H_2O$. JCPDF: 87-0720.

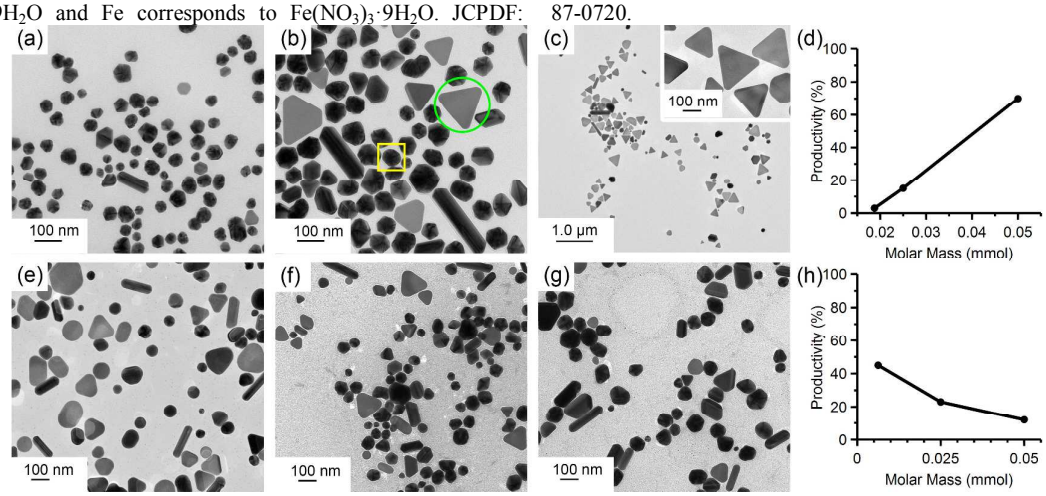

Figure 3. TEM images of AgNPs contained nanoplates (marked with circle) and twinned particles (marked with square) with different concentration of Al^{3+} ions and Fe^{3+} ions. (a) 0.01875mmol $Al(NO_3)_3$; (b) 0.025mmol $Al(NO_3)_3$; (c) 0.05mmol $Al(NO_3)_3$; (d) productivity of nanoplates in the presence of different concentration of Al^{3+} ions; (e) 0.00625mmol $Fe(NO_3)_3$; (f) 0.025mmol $Fe(NO_3)_3$; (g) 0.05mmol $Fe(NO_3)_3$; (h) productivity of nanoplates in the presence of different concentration of Fe^{3+} ions.

Figure 1d illustrates that TEM images in the presence of $Mg(NO_3)_3 \cdot 6H_2O$, with Ag nanoparticles obtained.

The X-ray diffraction (XRD) pattern of nanoparticles generated in different condition (as marked) was also carried out to identify the composition and purity, the results are shown in Figure 2. Using the face-centered cubic (fcc) structured reference pattern JCPDF: 87-0720[25], we indexed the peaks from left to right, they were {111}, {200}, {220} and {311}. The identification of the element composition was prepared with electron probe X-ray micro-analysis (EPMA) and plasma atomic emission spectroscopy (ICP-AES), as shown in Table 1. The molar ratios between Ag, Al and Fe were almost unanimously, and we suggest that little amount of Al in EPMA was induced by the Lα1 diffraction peak at 90.265 mm, which is similar to the Kα1 diffraction peak at 90.629 mm. This analysis shows that the final sample contained no Al or Fe element.

Additive	Analyzed molar ratios (Ag-Al-Fe) by EPMA	Analyzed molar ratios (Ag-Al-Fe) by ICP-AES
PVP	0.995：0.005：0	1：0：0
PVP+Al	0.994：0.006：0	1：0：0
PVP+Al+Fe	0.993：0.007：0	1：0：0
PVP+Fe	0.994：0.006：0	1：0：0

Table 1: Composition of prepared AgNPs.

To exclude the impact of anions contained in metal salts, we also repeated similar experiments with sulfates, acetates, etc. The TEM graphics of products in the presence of $Fe_2(SO_4)_3$ and $Al_2(SO_4)_3 \cdot 18H_2O$ are shown in Figure S1, the Ag nanoplates can be both notably observed. From the above experiments, it can be inferred that the Fe^{3+} ions and Al^{3+} ions have an specific effect on the nucleation and growth process of silver nanocrystals, resulting in the formation of silver plate-like structure.

A systematic and detailed study was carried out to illuminate the effect of Fe^{3+} and Al^{3+} on the Ag NCs nucleation and growth. Firstly, the concentration of metal ions was found to significantly affect both the morphology and the yield of Ag nanoplates. For the Al^{3+} ions, when the molar mass of Al^{3+} ions was increased from 0.00625 mmol (Figure 3a) to 0.025 mmol (Figure 3b), the yield of triangular nanoplates raised from ca.3% to ca. 15%. As the concentration up to 0.05mmol, the yield of nanoplates can reach to 70% (Figure 3c). Considering the addition of Fe^{3+} ions, when the concentration of Fe^{3+} ions was increased in the similar way (0.01875 mmol in Figure 3e, 0.025mmol in Figure 3f and 0.05mmol in Figure 3g), the productivity of nanoplates dropped gradually, from ca. 45% to ca. 12%. We attempted to decrease the concentration of Fe^{3+} ions in the solution. It was found that when the concentration was as low as 0.0025 mmol, the yield with Fe^{3+} ions could reach to 70%, as shown in figure S2a. The average edge length of the triangular plates is about 200 nm (Figure S2b) with various curvatures (Figure S2a).

From the experimental results obtained, we discoveryed that Fe^{3+} ions and Al^{3+} ions have a significant impact on the morphology of Ag NCs and could facilitate the plate-like nanostructure with PVP as stabilizer. By controlling their concentration and ratios in the reaction solution, we can successfully synthesize high-yielding silver triangular nanoplates. Comparing the concentration-productivity curve of Al^{3+} ions system and Fe^{3+} ions system displayed in Figure 3d and Figure 3h, we found that their concentration alteration have totally different effect, two different mechanism have been proposed then. As shown in Figure 3a-3c, it is obvious that the productivity of Ag nanoplates could be improved through improving the concentration of Al^{3+} ions in reaction solution. We speculated that Al^{3+} ions could play as a capping agent, which preferentially adhere to {111} facets. With increasing concentration, more {111} facets have been block, then the growth rate of other facets like {100} was enhanced, finally Ag nanoplates would be synthesized. Further researches would be carried out on the mechanism. In the previous researches, Fe^{3+} ions were usually used to promote the formation of Ag nanowires in the polyol reduction of silver nitrate[26]. Based on our observation, the addition of Fe^{3+} has promoted the formation of plate-like structure. The productivity of nanoplates is increased with the decrease of the concentration of Fe^{3+} ions, and the amount of the final structures of nanodisks or truncated nanoplates are considerable. It can be hypothesized that Fe^{3+} could oxidize Ag^0 back to Ag^+, thus reducing the super saturation of Ag atoms, therefore the kinetics during the nucleation and growth process had

been altered. However, as the concentration of Fe^{3+} increases, the ratio of nanoplates in final product dropped. It can be inferred that high concentration of Fe^{3+}

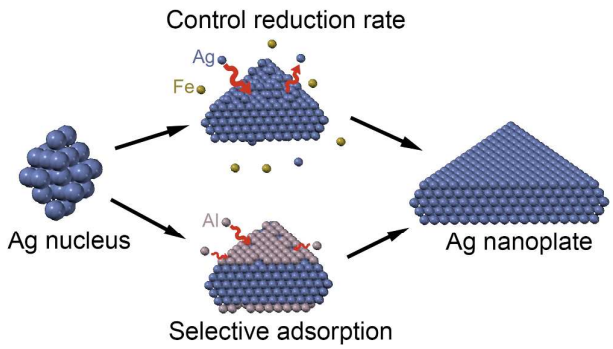

Figure 4. Schematic illustration of the evolution process of Ag nanoplates in the presence of Al^{3+} ions and Fe^{3+} ions: Fe^{3+} ions alter kinetics during reduction via oxidizing Ag^0 to Ag^+; Al^{3+} ions promote the nanoplates through preferential adsorption.

could promote the benzyl alcohol to reduce Fe^{3+} to Fe^{2+}, which could in turn remove oxygen from the surface of Ag atoms[26], then more multiply twinned nanoparticles were formed. The illustration of the mechanism underlying the influence of these two ions is displayed in Figure 4.

To further improve the yielding of plate-structured Ag NCs, we tried to add Al^{3+} ions and Fe^{3+} ions simultaneously, which combined the controlling kenetic and special absorption together. Figure 4a shows the typical transmission electron microscopy (TEM) images of Ag nanocrystallines in the presence of $Fe(NO_3)_3{\cdot}9H_2O$ and $Al(NO_3)_3{\cdot}9H_2O$. From which, we can obviously see that the final products are mainly triangular plates, whose size was ranging from 100 nm to 200 nm and the productivity of the nanoplates has reached up to 80%. Detailed characterization of the nanostructure obtained by the combination of Al^{3+} and Fe^{3+} ions was exhibited employing the high-resolution TEM and selected area electron diffraction (SAED) approaches. As shown in the inset of Figure 4b, a typical electron diffraction (ED) pattern was recorded by directing the electron beam perpendicular to the top faces of an individual nanoplate (Figure 4b). The six-fold rotational symmetry of the diffraction spots implies that the triangular faces are actually presented by {111} planes. Three sets of spots can be indentified based on the d-spacing: the spots (marked with the circle) with the

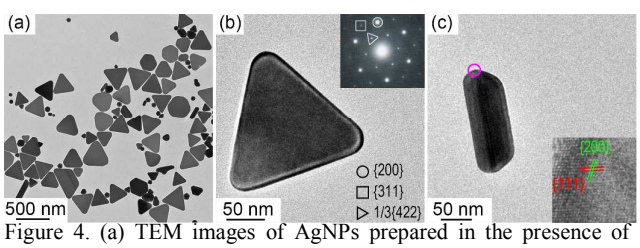

Figure 4. (a) TEM images of AgNPs prepared in the presence of PVP, 0.0025mmol $Fe(NO_3)_3$ and 0.0025mmol $Al(NO_3)_3$. (b) Corresponding individual nanoplate. Inset shows ED pattern taken from it by directing the electron beam perpendicular to its triangular faces. The strongest spots (circle) could be indexed to the {220} reflections, the outer spots (square) could be assigned to the {311} reflections, and the inner spots (triangle) corresponded to the formally forbidden 1/3{422} reflections. (c) The side of an individual triangular nanoplate and corresponding HRTEM image, Inset shows the lattice fringes. The triangular nanoplate was selected randomly.

strongest intensity could be indexed to the {220} reflections of fcc silver with a responding lattice spacing of 1.441 Å. The inner spots (marked with the triangle) with a weaker intensity is believed to be resulted from the formally forbidden 1/3{422} reflections and the outer set is related to the {311} planes of fcc silver. The inset in figure 4c is the high-resolution TEM image of the nanoplate recorded from the side face of an individual nanoplate. The red fringes could be indexed to {111} reflections, while the lattice spacing is measured to be 2.31 Å. The green fringes could be indexed to {200} reflection. These above assignment is consistent with some earlier researches, in which nanoplates are reported to be bounded by two {111} planes as the top and bottom faces and a mix of {100} and {110} planes as the side faces[27].

Conclusions

In summary, we systematically investigate the effect of foreign metal ions on the formation of Ag nanocrystals. In our developed BnOH-based synthetic system, Al^{3+} ions or Fe^{3+} ions could lead to the produce of silver nanoplates, while Ag nanoparticles were obtained in the presence of other metal ions (Mg^{2+}, Al^{3+}, Fe^{3+}, Ni^{2+}, Zn^{2+}, Zr^{4+}, etc.). We proposed that Al^{3+} ions promote the nanoplates through preferential adsorption while Fe^{3+} ions alter kinetics during reduction. By the assistance of the improved understanding of the roles of foreign metal ions, the investigation in present work allows us to shed new light on the underlying mechanism of the formation of structural architectures of silver nanoparticles.

Acknowledgements

The work was financially supported by the National Natural Science Foundation of China (51305225,51321092), the National Key Basic Research Program of China (2013CB934204).

Notes and references

[a] State Key Laboratory of Tribology, Beijing 100084, China.
[b] Department of Chemistry, Tsinghua University, Beijing 100084, China.

1 V. Voliani, F. Ricci, S. Luin and F. Beltram, J Mater Chem, 2012, 22, 14487-14493.
2 V. Voliani, G. Signore, O. Vittorio, P. Faraci, S. Luin, J. Peréz-Prieto and F. Beltram, Journal of Materials Chemistry B, 2013, 1, 4225-4230.
3 M. Liu, M. Leng, C. Yu, X. Wang and C. Wang, Nano Research, 2010, 3, 843-851.
4 Y. Sun and R. Qiao, Nano Research, 2008, 1, 292-302.
5 F. Xie, J. S. Pang, A. Centeno, M. P. Ryan, D. J. Riley and N. M. Alford, Nano Research, 2013, 6, 496-510.
6 D. Zhang, X. Liu and X. Wang, J Mol Struct, 2011, 985, 82-85.
7 K. E. Korte, S. E. Skrabalak and Y. Xia, J. Mater. Chem., 2008, 18, 437-441.
8 Y. Xia, Y. Xiong, B. Lim and S. E. Skrabalak, Angewandte Chemie International Edition, 2009, 48, 60-103.
9 L. Zhao, K. L. Kelly and G. C. Schatz, The Journal of Physical Chemistry B, 2003, 107, 7343-7350.
10 A. Panáček, L. Kvitek, R. Prucek, M. Kolar, R. Vecerova, N. Pizurova, V. K. Sharma, T. Nevečná and R. Zboril, The Journal of Physical Chemistry B, 2006, 110, 16248-16253.
11 I. Pastoriza-Santos and L. M. Liz-Marzan, J Mater Chem, 2008, 18, 1724-1737.
12 J. T. Zhang and X. M. Sun, J Phys Chem B, 2005, 109, 12544-12548.

13 J. E. Millstone, G. S. Metraux and C. A. Mirkin, Small, 2009, 5, 646-664.
14 P. Alivisatos, Nat Biotechnol, 2004, 22, 47-52.
15 E. C. Hao and J. T. Hupp, J Am Chem Soc, 2002, 124, 15182-15183.
16 Y. G. Sun, Small, 2007, 3, 1964-1975.
17 R. C. Jin, C. A. Mirkin and G. C. Schatz, Science, 2001, 294, 1901-1903.
18 R. C. Jin, E. C. Hao and G. C. Schatz, Nature, 2003, 425, 487-490.
19 C. Xue, Angew Chem Int Edit, 2007, 46, 2036-2038.
20 Y. J. Xiong, J. G. Wang and M. J. Kim, J Mater Chem, 2007, 17, 2600-2602.
21 Y. J. Xiong, J. Y. Chen and Z. Y. Li, J Am Chem Soc, 2005, 127, 17118-17127.
22 J. Y. Chen and Y. N. Xia, Angew Chem Int Edit, 2005, 44, 2589-2592.
23 I. Washio and Y. D. Yin, Adv Mater, 2006, 18, 1745.
24 B. Wiley and Y. N. Xia, Langmuir, 2005, 21, 8077-8080.
25 Powder Diffraction File (PDF), International Center for Diffraction Data (ICDD), formerly JCPDS, Newtown Square PA, USA.
26 Z. L. Wang, J Phys Chem B, 2000, 104, 1153-117